JOURNAL OF CATALYSIS 99, 53–61 (1986)

Temperature-Programmed Desorption Studies of Alcohol Decomposition on ZnO: 1-Propanol, 1-Butanol, and 2-Butanol

M. BOWKER, R. W. PETTS, AND K. C. WAUGH

New Science Group, ICI PLC, P.O. Box 11, The Heath, Runcorn, Cheshire WA7 4QE, United Kingdom

Received May 17, 1985; revised October 31, 1985

The adsorption and decomposition of 1-propanol, 1-butanol, and 2-butanol on polycrystalline ZnO has been investigated using temperature-programmed desorption (TPD). All three adsorb to a coverage of 2–5 × 10^{14} molecules cm^{-2} and decompose upon temperature programming to yield both dehydrogenated (aldehyde or ketone) and dehydrated (alkene) products into the gas phase. The peak decomposition rate is the same for both 1-ols (~545 K) and the same as for ethanol found in earlier work; 2-butanol decomposes 55 K lower, the same temperature as found for 2-propanol in previous work. It is proposed that this effect is due to alkoxide dehydrogenation rate-limiting the whole decomposition and that the transition state in the reaction involves a carbonium ion-like species; the secondary carbonium ion is more stable than the primary, thus resulting in the lower activation energy barrier for 2-ol decomposition. The selectivity for decomposition of the alcohols studied here favours the dehydrogenated product, as for 2-propanol, whereas in contrast, ethanol is 90% selective to dehydration. The near coincident peak temperature for dehydrogenated and dehydrated products in all cases is considered to be due to a two-step decomposition mechanism, namely (i) rate-limiting alkoxide dehydrogenation at the α-carbon atom yielding aldehyde/ketone into the gas phase and adsorbed hydride followed by (ii) hydride attack at the β-carbon hydrogen to yield hydrogen and alkene into the gas phase.

INTRODUCTION

In previous studies the interaction of methanol (*1*), ethanol (*2*), and 2-propanol (*3*) with the surface of a finely divided ZnO powder has been investigated. Methanol behaves very differently from the other alcohols, in that it reacts with the surface to form a strongly bound formate species. Ethanol and 2-propanol both decompose on the ZnO surface to yield dehydrogenated and dehydrated products upon temperature programming. However, though broadly similar in their behavior, there are significant differences between these two molecules; 2-propanol decomposes at 490 K to yield propylene and mainly acetone (65% selectivity), whereas ethanol decomposes at a higher temperature to yield predominantly ethylene (90%) (*3*). The reactive intermediate involved in these decompositions appears to be an alkoxide-like species which is associated with two different sites on the surface which evolve the two products.

The aim of the present study is to extend the earlier work with a view to making more generalised statements about the nature of alcohol decomposition on this surface, in particular to find out if there is a general trend of decomposition temperature within the alcohol series (as has been seen on metallic surfaces, for instance (*4*)) and likewise to investigate trends (if any) in the decompositional selectivity within the series. Thus, the adsorption of 1-propanol, 1-butanol, and 2-butanol on AnalaR ZnO has been studied and the results of this work are presented below.

EXPERIMENTAL

The equipment used has been described in detail in previous papers (*1–3*). Briefly, it consists of an adsorption chamber which contains the ZnO catalyst sample, the analysis chamber which houses a Vacuum Gen-

0021-9517/86 $3.00

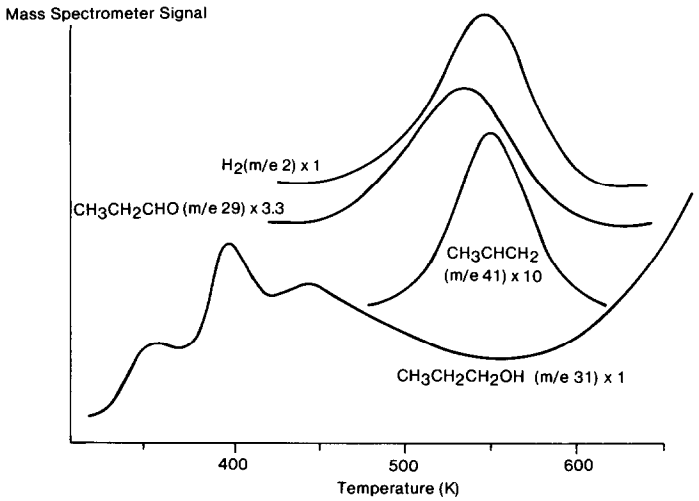

FIG. 1. Temperature-programmed desorption product distribution after the adsorption of 1-propanol on ZnO at 310 K. The spectra for individual masses are offset for clarity.

erators QX200 quadrupole mass spectrometer (and is separated from the adsorption chamber by a wide-bore valve so that the two chambers can be isolated from one another during dosing) and a gas line connected to the adsorption chamber by a fine leak valve. The sample of Analar ZnO (0.2 g; 3 m^2g^{-1} surface area; BDH Chemicals, Poole, England) was held in a quartz tube which could be heated to 850 K, using a temperature programmer. As noted in a previous paper (*5*) this ramp is not completely linear up to 400 K, but is completely linear after that. The heating rate used in this work was 0.52 K s^{-1}. Before the first experiments the sample was degassed at 670 K to remove volatile impurities such as H_2O and CO_2 (*1*), which constitute the major part (0.28%) of the impurity in the 99.7% pure sample. The sample was then reduced in H_2 for 15 min at 550 K to maintain the sample in a reproducibly defected state (*1*). The alcohols (Analar grade, 99.5% pure, BDH Chemicals Ltd.) were purified by freezing, thawing, and pumping cycles and their purity was confirmed by both the vapour pressure above the liquid and by their fragmentation patterns in the mass spectrometer. The alcohols were dosed at ambient temperature.

RESULTS

(*a*) *1-Propanol*

After propanol dosing at 310 K, the desorption product spectrum shown in Fig. 1 was obtained upon temperature programming. The products are the parent alcohol itself, desorbing in the low-temperature region (300–500 K) and characterised by major peaks at 31, 29, and 27 amu. Because of the deviation from linearity of the heating rate in this temperature region the desorption looks multipeaked, whereas there is probably only a single peak present. The temperature profile is completely linear after 400 K. After this desorption, evidence of the decomposition of a more strongly held species is seen, with the desorption peaking at ~540 K. The products are hydrogen, propylene (41, 42, 39, 27 amu are major peaks) and propionaldehyde (29, 28, 79, and 58 amu); there was no sign of other reaction products such as CO_2 or H_2O. It is noticeable in Fig. 1 that the aldehyde product peaks slightly before the other two products (by ~13 K), similar to the decomposition characteristics seen for 2-propanol (*3*). The desorption peak of propylene is also much narrower than that of propionaldehyde (FWHM of 45 vs 72 K, re-

TABLE 1

Alcohol Decomposition Parameters on Analar ZnO

Alcohol	Total coverage/alkoxide coverage (molecules $cm^{-2} \times 10^{-14}$)	Decomposition temperature (K) Aldehyde-ketone/alkene	E_d[a] (kJ mol^{-1})	E_d[b] (kJ mol^{-1})	Alkene selectivity
Ethanol	1.9/1.1	543/543	151	53	0.91
1-Propanol	4.5/1.2	537/551	148/152	52	0.28
2-Propanol	2.2/1.4	477/491	132/136	45	0.36
1-Butanol	5.5/1.5	538/550	149/152	52	0.43
2-Butanol	3.1/2.2	484/494	134/137	46	0.17

[a] Calculated from peak temperature assuming first-order preexponential factor of 10^{13} s^{-1}.
[b] Calculated assuming 10^{3} s^{-1} preexponential factor.

spectively) while the hydrogen peak has a width between these two (~60 K).

The amounts of material adsorbed for this saturation dose of *n*-propanol are calculated from the integral under the desorption peak making use of the sensitivity of the instrument to the particular desorbate and the pumping speed of the machine (1 litre s^{-1}) (*3*). The resulting coverages are given in Table 1. Also in Table 1 is the activation energy for desorption/decomposition for the two main desorption regions and this is calculated using Redhead's equation (*6*) as outlined elsewhere (*7*) and is discussed later in the paper. These data can be compared with the results for ethanol (*2*) and 2-propanol (*3*) which are also given in Table 1. The TPD experiments with these two molecules were repeated in this work and showed a difference in peak temperature for ethanol compared with the earlier study (*2*). The peak temperature was found to be that given in Table 1, 30 K higher than in the earlier report. The source of this discrepancy is not clear, but the series of data obtained in the present work were self-consistent. It is clear that 1-propanol decomposes at an almost identical temperature to ethanol, although the product ratio is very different, while 2-propanol decomposes ~60 K lower in temperature but has a similar product ratio to 1-propanol.

(*b*) *1-Butanol*

1-Butanol was dosed onto the ZnO sample at 310 K and the product distribution shown in Fig. 2 was obtained upon temperature programming. Once again the desorption pattern was similar to that seen for the other alcohols, that is, the desorption of parent 1-butanol (major peaks at 31, 56, 41, and 43 amu) in the low-temperature region (300–500 K), with evidence for the decomposition of a more strongly bound species at ~540 K. This more strongly held surface intermediate broke down to yield butyraldehyde (27, 29, 44, and 43 amu) and butene (41, 56, 39, and 27 amu) into the gas phase (exactly which isomer of butene it was we were not able to determine, since the fragmentation patterns of the butenes are very similar (*8*)). As described above for 1-propanol, the aldehyde product was observed to peak at ~13 K earlier than the alkene and had a much broader peak shape (FWHM of 72 K vs 60 K). The decomposition temperature was very similar to ethanol and 1-propanol, and product ratios, coverages, and decomposition activation energies are given in Table 1.

(*c*) *2-Butanol*

The desorption spectrum seen upon heating the ZnO sample which had been dosed with 2-butanol at 310 K is shown in Fig. 3.

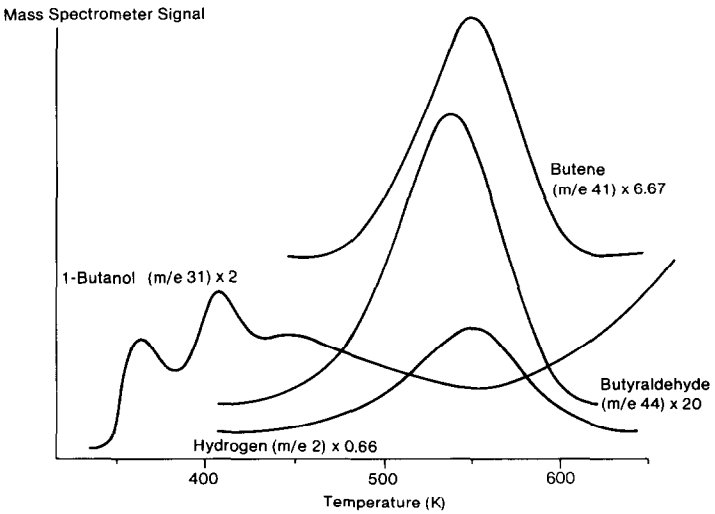

FIG. 2. Temperature-programmed desorption product distribution after 1-butanol adsorption on ZnO at 310 K. The spectra are offset vertically for clarity.

As for all the other alcohols there are two regimes of desorption: the parent alcohol (45, 59, 31, and 27 amu) desorbs at relatively low temperatures ($T_p \sim 420$ K) and a more strongly bound species decomposes to yield 2-butanone (43, 29, 72, and 27 amu), butene (masses as above), and hydrogen. At this stage of the study the heating rate had become much closer to linear in the lower temperature regime so that the desorption of the 2-butanol looks more "normal" than in the cases above. The decomposition of the strongly bound intermediate occurs at about 490 K, identical to that for the other branched alcohol previously studied, 2-propanol, and very much lower (by 60 K) than the straight-chain alcohols. Once again the dehydrogenated product peaks before the dehydrated product, in this case by ~10 K. The other

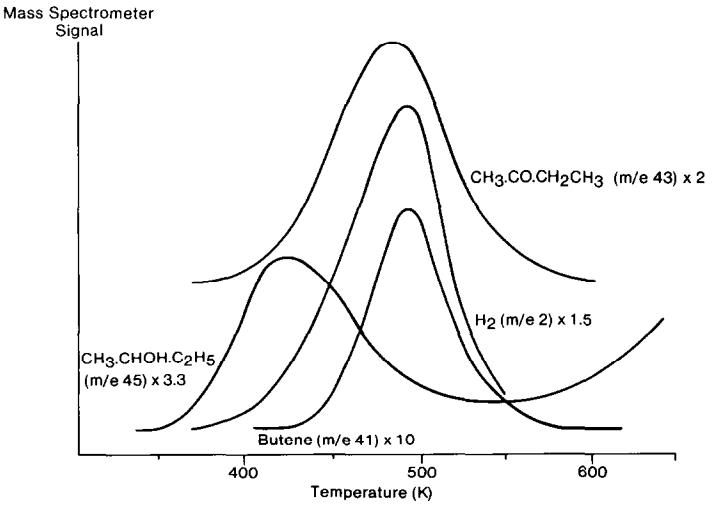

FIG. 3. Temperature-programmed desorption product distribution after 2-butanol adsorption on ZnO at 310 K. The spectra are offset vertically for clarity.

parameters relating to 2-butanol adsorption and decomposition are presented in Table 1.

DISCUSSION

Having reported the adsorption and reaction of six alcohols with the ZnO surface, both in this work and earlier papers (*1–3*), a general mechanism for the decomposition of all the alcohols except methanol (which appears to behave in an "anomalous" way) can be written as follows:

Adsorption at 310 K	$HR\!>\!CHOH_{(g)}$ (R′)	$\rightarrow HR\!>\!CHOH_{(a)}$ (R′)	(1)
Reaction with surface at 310 K	$HR\!>\!CHOH_{(a)}$ (R′)	$\rightarrow HR\!>\!CHO_{(a)} + H_{(a)}$ (R′)	(2a)
	$HR\!>\!CHOH_{(a)} + O_{(s)}$ (R′)	$\rightarrow HR\!>\!CHO_{(a)} + OH_{(a)}$ (R′)	(2b)
	$2H(a)$	$\rightarrow H_{2(g)}$	(3a)
	$H_{(a)} + OH_{(a)}$	$\rightarrow H_2O_{(g)} + V_O^{2-}$	(3b)
Desorption (300–500 K)	$HR\!>\!CHOH_{(a)}$ (R′)	$\rightarrow HR\!>\!CHOH_{(g)}$ (R′)	(4)
Decomposition at 500–550 K	$HR\!>\!CHO_{(a)}$ (R′)	$\rightarrow HR\!>\!C{=}O_{(g)} + H_{(a)}$ (R′)	(5a)
	$HR\!>\!CHO_{(a)} + H_{(a)} + V_O^{2-}$ (R′)	$\rightarrow R{=}\overset{H}{\overset{\vert}{C}}{-}R'_{(a)} + O_{(s)} + H_{2(g)}$	(5b)
	$R{=}\overset{H}{\overset{\vert}{C}}{-}R'_{(a)}$	$\rightarrow R{=}\overset{H}{\overset{\vert}{C}}{-}R'_{(g)}$	(6)
	$2H(a)$	$\rightarrow H_{2(g)}$	(7)

Adsorption step (1) proceeds slowly and so it is likely to be activated. Dissociation of the alcohol probably takes place upon adsorption and steps (2b) and (3b) are inferred from the fact that, even when prereduction of the sample was not used, the decomposition pattern was reproducible, that is, even though oxygen is being stripped from part of the adsorbate [step (5b)] the surface does not "block up" with oxygen and the adsorption features remain unchanged. Thus the O_s released in step (5b) must be lost in a reaction upon adsorption [steps (2b, 3b)] since no water is seen in the desorption products during temperature programming. Likewise steps (2a) and (3a) probably occur upon adsorption since no hydrogen is seen in the low-temperature desorption region; the possibility of hydrogen recombination below 310 K on ZnO has been demonstrated by Griffin and Yates (*9*). Step (4) represents the desorption of unreacted alcohol which leaves the strongly bound alkoxide intermediate on the surface. How-

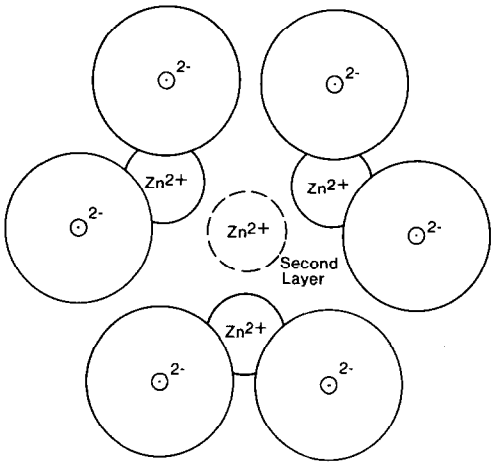

FIG. 4. The idealised (000$\bar{1}$) polar surface of ZnO with an anion vacancy present which leaves zinc ions exposed. The atoms are drawn with their normal divalent radii, but the two electrons associated with the defect may be localised at adjacent zinc ions giving small polarons, effectively Zn^+ ions.

ever, two types of alkoxide are postulated, one next to an anion vacancy V_O^{2-} and one at an unperturbed site (assuming that the alkoxide is primarily attached to the surface via the oxygen end of the molecule at cation sites, which is the kind of mode seen on metallic surfaces (*4*)). The mechanism of the decomposition is then different for the two types of species; the former "heals" the defect to produce alkene, while the latter produces the aldehyde/ketone. It is somewhat surprising, therefore, that the kinetics of decomposition of the two are so nearly identical; the 10 K or so difference in peak temperatures only represents an energy difference of ~3 kJ mol^{-1} for two independent processes. This will be discussed further below.

The different sites proposed above may be associated with crystallographic anisotropy of the catalytic reactivity of ZnO surfaces, as noted previously for other molecules (*10, 11*). In particular, it may be that the dehydrogenation reaction described above is located at sites on the (0001) polar face, which has the same geometry as that shown in Fig. 4 and has a surface of exposed Zn ions, possibly even Zn^+ ions (*12*). This metallic-like phase could then behave in a similar manner to copper surfaces (*4*), carrying out the dehydrogenation reactions on the alcohols. Indeed, the surface coverage by these kinds of species is close to that of the density of such polar sites in the ZnO sample (~11×10^{13} atoms cm^{-2} of total catalyst area). The other sites are then either associated with polar (000$\bar{1}$) faces or with the prism planes. The type of defect site with which the species could be associated is shown in Fig. 4. In this case the exposed central defect site is likely to be either a substitutional Zn^+ ion with an electron localised in the oxygen vacancy (F centre), or it is possible that both electrons from the missing oxygen are localised on zinc ions giving two substitutional Zn^+ species (small polarons) (*13*). The alkoxide species associated with these defects is probably more stable than the other alkoxides. However, it reacts on decomposition to produce the alkene by β-H elimination/abstraction by the hydride species produced in step (5a). This mechanism is almost identical to that already proposed by Ashby *et al.* for the thermal decomposition of zinc dialkoxides (*14*), the main difference being that in the dialkoxide case the hydride is located on the same zinc atom as the original two alkoxides, whereas for the surface reaction described in this work the hydride must be somewhat mobile on the surface in order to move from production to reaction sites. The surface hydride may well be the polar species described by Griffin and Yates after the adsorption of hydrogen on ZnO (*15*).

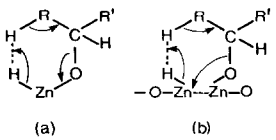

FIG. 5. (a) The transition state proposed by Ashby *et al.* (*14*) to be involved in the second step of zinc dialkoxide decomposition (hydride attack at the second alkoxide). (b) The transition state proposed in this work for the hydride-induced dehydration step of alkoxides on the ZnO surface.

TABLE 2

Modeling Parameters for Alkoxide Decomposition

Product	Reaction step	ν (s^{-1})	E (kJ mol^{-1})	T_p[a] (K)	FWHM[a] (K)
Aldehyde or ketone	α-CH cleavage, (5a) in text	10^3	52	535	100
Hydrogen	Hydride-induced alkoxide decomposition, (5b) in text	8×10^3	57	547	82
Hydrogen	Hydrogen recombination, (7) in text	2×10^3	48		
Alkene	Alkene desorption, (6) in text	10^{10}	117	547	44

[a] Parameters derived from desorption spectra produced by the computer model.

Ashby *et al.* (*14*) have described a six-centre transition state (t.s.) for the alkene production process, as shown in Fig. 5a. Whether the t.s. for the surface reaction we have described is exactly the same geometry as this is uncertain. It may be so, in which case the hydride has to diffuse to the very surface site at which the alkoxide is adsorbed. Perhaps more likely is that the alkoxide is attacked by the hydride from an adjacent cation site forming a t.s. with a dual cation site; this can be visualised as a seven-centre complex and is illustrated in Fig. 5b. The hydride diffusion presumably takes place from cation to cation, electrostatic repulsions resulting in anion avoidance.

The two-step mechanism of hydride production followed by β-H abstraction can be taken as an explanation for the similarity of decomposition temperatures for the two different alkoxyl species. The alkoxyl associated with an adjacent anion vacancy is probably considerably more strongly bound than the other species and it is the hydride reaction which breaks the C–O bond. The order of appearance of the dehydrogenated and dehydrated products is as expected from this mechanism and the small difference in decomposition temperatures was previously explained as due to an additional small activation energy for the hydride induced β-elimination/abstraction described above. Some estimation of this activation energy can be made using a computer program to derive the desorption curves from the above mechanism. No allowance has been made for possible readsorptive broadening in the spectra, but the parameters shown in Table 2 were used to generate the curves of Fig. 6. It was found that the basic tenet of "temperature-programmed reaction spectroscopy" as propounded by Madix (*16*) (that weakly held products evolving from a common rate-determining step desorb coincidently) held for this situation, that is, the temperature shift cannot be explained simply by a small additional reaction enthalpy for a sequential reaction [(5b) above being dependent on the occurrence of (5a)]. In fact an enthalpy comparable with that required to produce a desorption peak at that temperature is required to produce the small shift. As shown in Table 2, the great width of the peak due to the dehydrogenation reaction can only be simulated by using a very low desorption preexponential and a low reaction energy to compensate. The value chosen for ν for this reaction, 10^3 s^{-1}, is close to that found for bulk zinc alkoxide decompositions by Ashby *et al.* (*14*), as is the desorption energy. The values used for the other parameters have several constraints on them, viz. (i) fitting the peak temperature difference between aldehyde and alkene/hydrogen products,

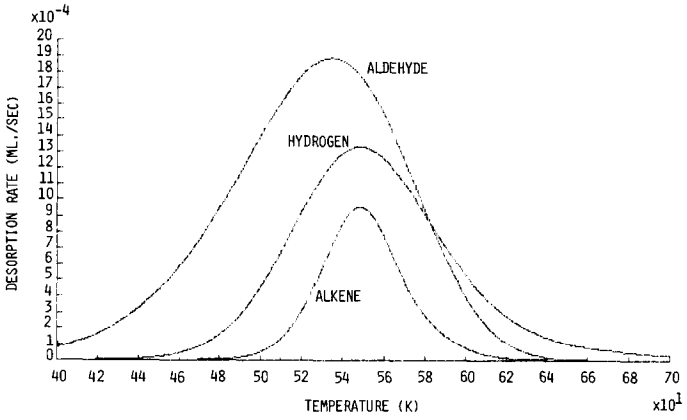

FIG. 6. Computer-simulated temperature-programmed desorption spectrum for alcohol decomposition. The curves were produced using the kinetic parameters given in Table 2.

(ii) fitting approximately the aldehyde/alkene ratio, and (iii) fitting the lineshapes. It is (i) and (iii) which determine the higher values of ν and E needed for alkene desorption. It is (ii), which determines the kinetic values for step (5b): too low a value for the rate constant and no alkene is formed at all, too high and the amount of alkene formed is too high. The higher values of ν and E for alkene loss from the surface imply a desorption-limited evolution which further implies a relatively strong binding of the alkene product to the ZnO surface. This latter point would be an interesting one to test experimentally. However, the purpose of the curve-fitting exercise described above was not to show exact quantitative results for the kinetics of the reaction scheme, but to show qualitatively that the reaction scheme is feasible in terms of the gross features of the desorption spectra reported.

Since these results and those of Ashby *et al.* (*14*) indicate that low values for ν and E are appropriate to this reaction system, Table 1 shows values for E determined using Redhead's Eq. (*6*) assuming values of ν of 10^3 and 10^{13} s^{-1}, the latter being the usual assumed value for desorption preexponential factors. The low value of ν determined from the curve-fitting agrees well with values determined by Carrizosa and Munuera (*18*) for alcohol dehydration reactions on titania.

The notable stability difference between the straight chain and branched alkoxide decomposition temperatures is probably related to the formation of some kind of carbonium ion-like transition state during step (5a). As shown in Fig. 7 below, the transition state (prior to hydride dissociation) could be a species with separated charges and a positively charged α-carbon atom. It is well known that such charge centres are stabilised by the presence of directly attached alkyl groups which push charge into the α-carbon (*17*). As a result secondary carbonium ions are more stable than pri-

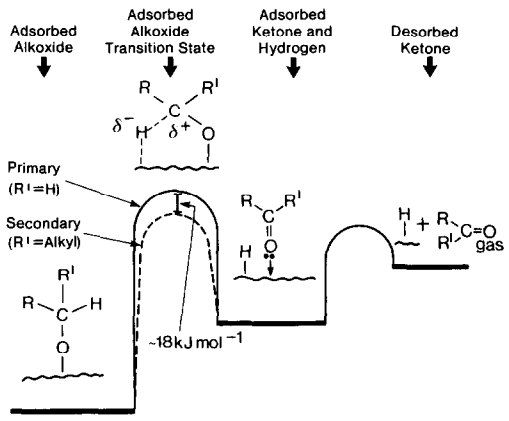

FIG. 7. Schematic one-dimensional potential energy profiles for alkoxide decomposition on ZnO illustrating the greater stability of the secondary carbonium-like transition state and resulting reduction of the energy barrier to alkoxide decomposition.

mary, as shown in Fig. 7, the transition state energy is lower and so the overall decomposition activity energy is reduced. Hence the lower peak temperature for the secondary alcohols shown in the present work. In fact, if the decomposition peak temperature is lower solely due to this effect, and it is only the energy parameter that is affected, then the stabilisation of these species on the surface (ΔE in Fig. 7) amounts to ~ 18 kJ mol^{-1}. This simple argument also explains why all the similar alcohols decompose at the same temperature, that is, the reactive centre is identical for all of them. Presumably, tertiary alkoxides would decompose at an even lower temperature, though the reaction mechanism would be very different from that shown in step (5) above, since there is no α-C hydrogen atom in that case.

The reason for the considerable difference of selectivity for ethanol is not clear. It may be that, as proposed in the earlier paper, there is much more interaction of the β-C with the surface in that case and that, as well as α-C hydrogen abstraction and resulting hydride reaction at the β-C, direct β-C hydrogen abstraction can occur at the surface. This must also be related to the adsorption reaction, since most must be adsorbed via steps (2b/3b) because 90% of the products seen at 540 K are due to dehydration and yet no water is desorbed during heating.

In this paper we have presented data from the use of only one experimental technique, temperature-programmed desorption, and, as might be anticipated from such a limited probe, several questions remain incompletely answered and will require the use of other techniques such as surface spectroscopy and microreactor measurements to clarify the situation. Nevertheless, from this series of experiments using TPD alone considerable insight has been gained into the reaction processes of alcohols on ZnO surfaces. In particular, the alcohols decompose in two steps, first by α-C–H bond scission yielding the dehydrogenation product into the gas phase and one adsorbed (and highly mobile) hydride species, and second by hydride-induced hydrogen stripping from the β-C to yield the dehydrated product and hydrogen into the gas phase, and inserting an oxygen atom into the lattice.

REFERENCES

1. Bowker, M., Houghton, H., and Waugh, K. C., *J. Chem. Soc., Faraday Trans. 1* **77,** 3023 (1981).
2. Bowker, M., Houghton, H., and Waugh, K. C., *J. Chem. Soc., Faraday Trans. 1* **78,** 2573 (1982).
3. Bowker, M., Petts, R., and Waugh, K. C., *J. Chem. Soc., Faraday Trans. 1* **81,** 3073 (1985).
4. Bowker, M., and Madix, R. J., *Surf. Sci.* **116,** 549 (1982).
5. Bowker, M., Houghton, H., and Waugh, K. C., *J. Catal.* **79,** 431 (1983).
6. Redhead, P., *Vacuum* **12,** 203 (1962).
7. Morris, M. A., Bowker, M., and King, D. A., *in* "Comprehensive Chemical Kinetics" (C. Bamford, C. F. H. Tipper, and R. Compton, Eds.), Vol. 19, p. 92, Elsevier, Amsterdam, 1984.
8. Cornu, A., and Massot, R., *in* "Compilation of Mass Spectral Data." Heyden, London, 1966.
9. Griffin, G., and Yates, J., *J. Catal.* **73,** 396 (1982).
10. Bowker, M., Houghton, H., Waugh, K. C., Giddings, T., and Green, M., *J. Catal.* **84,** 252 (1983).
11. Cheng, W., and Kung, H., *Surf. Sci.* **102,** L21 (1981).
12. Hirschwald, W., Bonasewicz, P., Ernst, L., Grade, M., Hofmann, D., Krebs, S., Littbarsky, R., Neumann, G., Grunze, M., Kolb, D., and Schultz, H., *in* "Current Topics in Material Science, Vol. 7" (E. Kaldis, Ed.), p. 155. Elsevier, Amsterdam, 1981.
13. Mackrodt, W., Stewart, R., Campbell, J., and Hillier, I., *J. Phys. (Paris)* **41,** C6 (1980).
14. Ashby, E., Willard, G., and Goel, A., *J. Org. Chem.* **44,** 1221 (1979).
15. Griffin, G., and Yates, J., *J. Chem. Phys.* **77,** 3744 (1982).
16. Madix, R. J., "Advances in Catalysis," Vol. 29, p. 1. Academic Press, New York, 1980.
17. Morrison, R., and Boyd, R., "Organic Chemistry," 2nd ed., p. 165. Allyn and Bacon, Boston, 1969.
18. Carrizosa, I., and Munuera, G., *J. Catal.* **49,** 174, 189 (1977).